Original Article

Application of the Kaiser score on contrast-enhanced mammography in the differential diagnosis of breast lesions: comparison with breast magnetic resonance imaging

Xiaocui Rong^, Yihe Kang, Yanan Li, Jing Xue, Zhigang Li, Guang Yang^

Department of Radiology, The Fourth Hospital of Hebei Medical University, Shijiazhuang, China

Contributions: (I) Conception and design: X Rong, Y Kang, G Yang; (II) Administrative support: Z Li, G Yang; (III) Provision of study materials or patients: Y Li, J Xue; (IV) Collection and assembly of data: Y Kang; (V) Data analysis and interpretation: X Rong; (VI) Manuscript writing: All authors; (VII) Final approval of manuscript: All authors.

Correspondence to: Guang Yang, MD. Department of Radiology, The Fourth Hospital of Hebei Medical University, 12 Jian-kang Rd., Shijiazhuang 050011, China. Email: yanggzj@163.com.

Background: The Kaiser score (KS) as a clinical decision rule has been proven capable of enhancing the diagnostic efficiency for suspicious breast lesions and obviating unnecessary benign biopsies. However, the consistency of KS in contrast-enhanced mammography (CEM-KS) and KS on magnetic resonance imaging (MRI-KS) is still unclear. This study aimed to evaluate and compare the diagnostic efficacy and agreement of CEM-KS and MRI-KS for suspicious breast lesions.

Methods: This retrospective study included 207 patients from April 2019 to June 2022. The radiologists assigned a diagnostic category to all lesions using the Breast Imaging Reporting and Data System (BI-RADS). Subsequently, they were asked to assign a final diagnostic category for each lesion according to the KS. The diagnostic performance was evaluated by the area under the receiver operating characteristic curve (AUC). The agreement in terms of the kinetic curve and the KS categories for CEM and MRI were evaluated via the Cohen kappa coefficient.

Results: The AUC was higher for the CEM-KS category assignment than for the CEM-BI-RADS category assignment (0.856 *vs.* 0.776; P=0.047). The AUC was higher for MRI-KS than for MRI-BI-RADS (0.841 *vs.* 0.752; P =0.015). The AUC of CEM-KS was not significantly different from that of MRI-KS (0.856 *vs.* 0.841; P=0.538). The difference between the AUCs for CEM-BI-RADS and MRI-BI-RADS was not statistically significant (0.776 *vs.* 0.752; P=0.400). The kappa agreement for the characterization of suspicious breast lesions using CEM-KS and MRI-KS was 0.885.

Conclusions: The KS substantially improved the diagnostic performance of suspicious breast lesions, not only in MRI but also in CEM. CEM-KS and MRI-KS showed similar diagnostic performance and almost perfect agreement for the characterization of suspicious breast lesions. Therefore, CEM holds promise as an alternative when breast MRI is not available or contraindicated.

Keywords: Breast neoplasms; contrast-enhanced mammography (CEM); magnetic resonance imaging (MRI); clinical decision support system; diagnosis

Submitted Mar 25, 2024. Accepted for publication Jun 20, 2024. Published online Jul 18, 2024.
doi: 10.21037/qims-24-593
View this article at: https://dx.doi.org/10.21037/qims-24-593

^ ORCID: Xiaocui Rong, 0000-0003-0325-296X; Guang Yang, 0000-0002-0922-3943.

Introduction

Breast cancer is the most common malignant tumor among women worldwide (1) and seriously endangers women's health. Breast magnetic resonance imaging (MRI) is considered to be the most sensitive examination method to detect breast cancer. However, some limitations that prevent a wider use of breast MRI persist, such as a relatively low specificity, high cost, extensive duration, and poor patient compliance. Contrast-enhanced mammography (CEM), which was first approved by the United States Food and Drug Administration (FDA) in 2011, represents a breakthrough in mammography in recent years and uses dual energy for mammographic acquisition with intravenous iodine contrast material. The recombined (RC) images are produced by postprocessing from high-energy and low-energy images, which are used to assess the tumor neoangiogenesis and to remove the overlap of surrounding normal gland tissues so that the lesions can be more clearly displayed. Previous studies have examined the diagnostic performance of CEM compared with MRI for the diagnosis of breast lesions, most of which demonstrated that CEM has comparable diagnostic performance to MRI and may even have a higher specificity (2-7).

The use of the Kaiser score (KS) as a clinical decision rule has been proven capable of enhancing the diagnostic efficiency for suspicious breast lesions and obviating unnecessary benign biopsies (8-13), with excellent interobserver agreement (10,14,15). The Breast Imaging Reporting and Data System (BI-RADS) is a common diagnostic tool in clinical work, which provides a lexicon of descriptors to standardize reporting, diminishes confusion in the interpretation of the imaging findings, and simplifies outcome monitoring (16). However, it lacks definite diagnostic criteria that can objectively and reliably exclude malignancy. The KS provides an intuitive tree flowchart based on five diagnostic criteria (spiculated sign, kinetic curve, internal enhancement characteristic, margin, and edema) to assign the score (17). The score ranges between 1 and 11, with a higher score indicating a higher probability of malignancy. Scores below 5 can generally be considered benign, while lesions with a KS of 5 or higher typically require a histological biopsy (18-20). Despite there being only a few studies on the diagnostic efficiency of the KS on CEM (CEM-KS), the preliminary results have been encouraging (12,13). However, the consistency of CEM-KS and KS in MRI (MRI-KS) is still unclear. Therefore, this study aimed to investigate and compare the diagnostic performance and agreement of CEM-KS and MRI-KS for suspicious breast lesions. We present this article in accordance with the STARD reporting checklist (available at https://qims.amegroups.com/article/view/10.21037/qims-24-593/rc).

Methods

Patients

This retrospective, a single-center study was approved by the ethics committee of The Fourth Hospital of Hebei Medical University (No. 2020ky182) and was conducted in accordance with the Declaration of Helsinki (as revised in 2013). The requirement for written informed consent was waived. From April 2019 to June 2022, consecutive patients with suspicious findings of the breast (BI-RADS 4-5) on digital breast tomosynthesis or ultrasound (US) and undergoing CEM and breast MRI in our institution were considered as candidates for this study. Only the index lesion confirmed by histopathology in each breast was chosen for analysis. The exclusion criteria in our study were as follows: (I) no pathological results (n=11), (II) no abnormal enhancement on CEM or MRI (n=7), and (III) chemotherapy or surgery before CEM or MRI (n=4). Finally, 207 patients were included in the analysis. The detailed workflow is shown in *Figure 1*. The clinical indications for the patients included in this study were as follows: a palpable lump (184/207, 88.9%), screening with abnormalities (17/207, 8.2%), and discharge from the nipple (6/207, 2.9%).

Imaging protocol

CEM procedure

CEM was performed using a dual-energy digital mammography (DM) system (Senographe Essential, GE HealthCare, Chicago, IL, USA) with an automatic exposure mode, which was equipped with an amorphous silicon flat panel detector and a field of view (FOV) of 24×31 cm and a pixel size of 100 μm. A filter composed of copper and aluminum was used for the high-energy acquisition of CEM, and a molybdenum or rhodium filter was used for the low-energy acquisition, which was the same as that for mammography. Intravenous iodinated contrast (370 mgI/mL) was administered at a dose of 1.22 mL/kg body weight and an injection rate of 3 mL/sec. Two minutes after administration of contrast, each breast projection was performed in the following order: craniocaudal (CC) nonaffected side, CC affected side at 3 minutes (early phase),

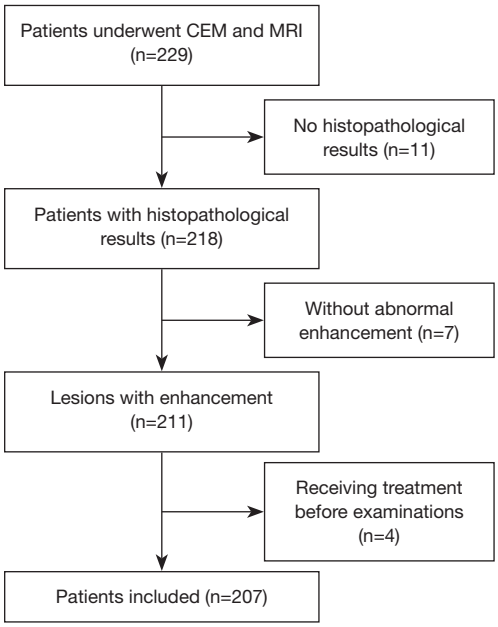

Figure 1 The flowchart of patient inclusion. CEM, contrast-enhanced mammography; MRI, magnetic resonance imaging.

mediolateral oblique (MLO) nonaffected side, and MLO affected side completed within 6 minutes. The delayed images of the CC affected side were acquired in 7–9 minutes after the injection of the contrast agent.

Breast MRI

Breast MRI was carried out on a 1.5-T (Signa HDe, GE HealthCare) or a 3-T (MAGNETOM Skyra, Siemens Healthineers, Erlangen, Germany) MR scanner with dedicated breast-surface coils. The 1.5-T dynamic contrast-enhanced (DCE) MRI was conducted using volume imaging for breast assessment (VIBRANTI) and fat-suppressed technology under the following parameters: repetition time (TR)/echo time (TE), 5.6/1.0 ms; flip angle, 15°; FOV, 32 cm; matrix, 320×288; slice thickness, 1.2 mm; slice gap, 0 mm; and acquisition time, 60 s. The dynamic series included 8 phases: one was obtained before and seven were obtained after a 20-second delay after the injection of the MRI contrast agent (gadoterate meglumine, 0.1 mmoL/kg body weight at a rate of 3 mL/sec).

The protocol for 3.0-T MRI included the following sequences: (I) axial T1-weighted imaging [T1-weighted imaging (T1WI); TR/TE, 6.04/2.46; FOV, 36 cm; slice thickness, 4 mm], (II) axial fat-suppressed T2-weighted imaging (T2WI) (TR/TE, 5,630/84; FOV, 35 cm; slice thickness, 4.5 mm), (III) axial fat-suppressed DCE T1WI (TR/TE, 4.31/1.61; FOV, 36 cm; slice thickness, 1.3 mm). One phase was scanned before the intravenous injection of the contrast agent. Dynamic-enhanced scanning was performed approximately 25 seconds after the injection of the contrast agent, and six uninterrupted scans were performed, with each scanning time lasting 75 seconds.

Imaging analysis

CEM image analysis

The CEM images were evaluated by two experienced radiologists who were unaware of the pathological results, and the final results were determined by discussion when there was a disagreement. First, the radiologists assigned a diagnostic category to all lesions using the 2022 CEM BI-RADS (21). Subsequently, they were asked to assign a final diagnostic category for each lesion according to the KS. Before starting the image analysis, the readers had studied the KS in depth (20).

The manifestations of breast enhancing lesions on CEM images were divided into mass and non-mass enhancement (NME). For the masses, their shape (round, oval, or irregular), margin (circumscribed, irregular, or spiculated), internal enhancement pattern (heterogeneous, homogeneous, or rim enhancement), and kinetic curves (increase in the enhancement intensity of the delayed lesion of more than 10% compared with the early phase was considered to be persistent, a change range of ±10% was considered to be plateau, and a decrease in enhancement intensity decrease of more 10% was considered to be washout) (22) were analyzed. NME was analyzed in terms of distribution (diffuse, multiple regional, regional, focal, linear, or segmental), internal enhancement pattern (homogeneous or heterogeneous), margin (circumscribed, irregular, or spiculated), and kinetic curve (washout, plateau, or persistent).

On the RC images, the region of interest (ROI) was manually delineated, and the percentage signal difference between the enhancing lesion and background (%RS) was calculated according to the following formula (23),

$$\%RS = \frac{s'c - s'b}{s'b} \times 100\% \quad [1]$$

where $s'c$ and $s'b$ are the mean signal of the ROI in the enhancing lesion and background, respectively, and $\%RS$ represents the enhancement intensity of the lesion.

Because CEM could not assess perifocal oedema, the average scores were taken as the KS score (9 or 10) when

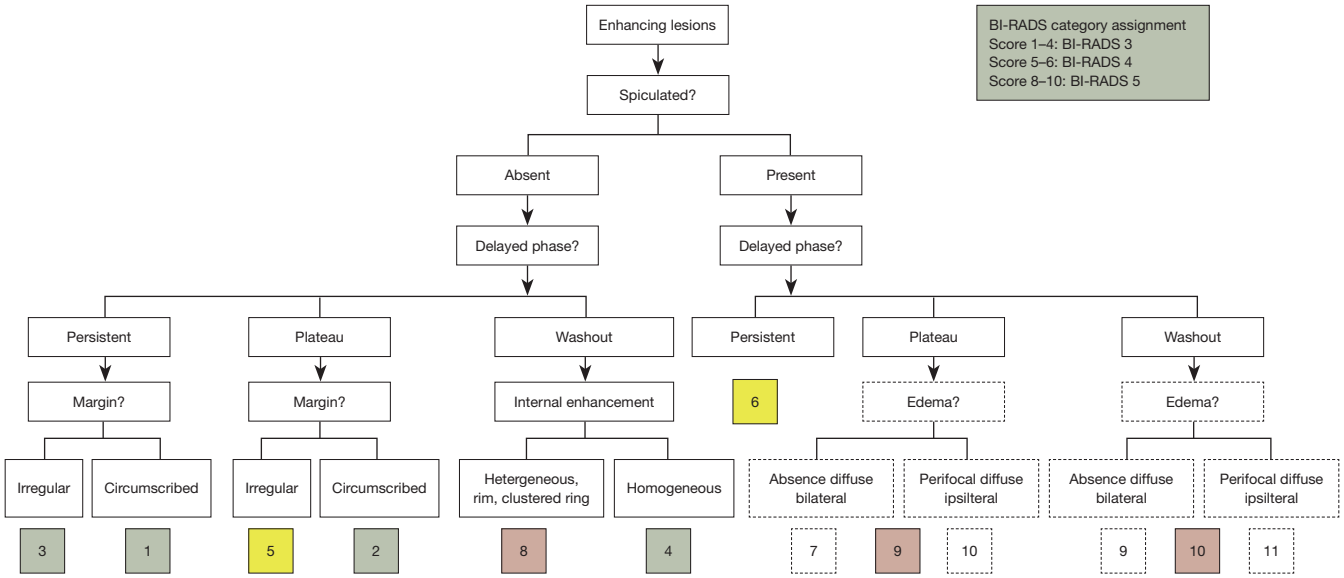

Figure 2 The KS flowchart of CEM. The diagnostic score is associated with an increasing probability of malignancy (1 = lowest, 10 = highest). BI-RADS, Breast Imaging Reporting and Data System; KS, Kaiser score; CEM, contrast-enhanced mammography.

the lesions were characterized by spiculated margins and plateau or washout curves (*Figure 2*).

MR image analysis

MRI was evaluated by an experienced reader blinded to the histopathological and other imaging results. First, the reader assigned a BI-RADS category to all lesions using the 2013 MRI BI-RADS (24). The reader then assigned a final diagnostic category for each lesion according to the KS (20).

Statistical analysis

Statistical analysis was performed using SPSS version 21.0 (IBM, Corp. Armonk, NY, USA) and MedCalc 11.4.2.0. The pathological results obtained by biopsy or surgery were taken as the gold standard. A receiver operating characteristic (ROC) curve analysis was performed, and the area under the ROC curve (AUC) was obtained to assess the diagnostic performance of CEM and MRI with BI-RADS and the KS. The DeLong test was used to compare the AUCs. The sensitivity, specificity, negative predictive value (NPV), positive predictive value (PPV), and positive likelihood ratio (+LR) and negative likelihood ratio (–LR) were calculated with 95% confidence intervals (CIs) based on BI-RADS category, with a cutoff value of ≥4 used to designate malignant lesions. The sensitivity and specificity on CEM and MRI were compared by using the McNemar test. The agreement in terms of the kinetic curve and the KS categories for CEM and MRI were evaluated with the Cohen kappa coefficient. In addition, the cost-effectiveness of CEM-KS and MRI-KS was evaluated via the cost: AUC ratio. For all tests, a P value <0.05 was considered to be statistically significant.

Results

Study population

A total of 208 lesions in 207 patients (age range, 21–74 years; mean age 48.39±10.36 years) were included in this study with 152 (73.1%, 152/208) malignant and 56 (26.9%, 56/208) benign lesions. The mean size of the malignant lesions (23.3±13.3 mm) was higher than that of the benign lesions (19.5±11.5 mm; P=0.015). Among the 208 lesions, 4 benign lesions and 7 malignant lesions were not visible on US, while 197 lesions were found to be abnormal on US. The patients included 85 postmenopausal and 122 premenopausal women. The pathological results of US-guided biopsy (n=10) and surgery (n=198) are listed in *Table 1*.

CEM and MRI characteristics

The manifestations of the breast lesions on CEM were distributed as follows: there were 147 masses and 61 cases

Table 1 Histopathological results of the study population

Pathology	Number of cases (%)
Benign	56 (26.9)
Adenosis	21 (37.5)
Intraductal papilloma	14 (25.0)
Fibroadenoma	13 (23.2)
Inflammatory disease or cyst with infection	4 (7.1)
Benign phyllodes tumor	2 (3.6)
Mucocele-like lesions	1 (1.8)
Myofibroblastoma	1 (1.8)
Malignant	152 (73.1)
Invasive ductal carcinoma	106 (69.7)
Ductal carcinoma in situ	27 (17.8)
Papillary carcinoma	9 (5.9)
Invasive lobular carcinoma	3 (2.0)
Mucinous carcinoma	2 (1.3)
Mixed carcinoma	3 (2.0)
Metaplastic carcinoma	1 (0.65)
Neuroendocrine tumor G2	1 (0.65)

of NME; moreover, there were 150 lesions that manifest as masses and 58 as NME on MRI. The distribution of the lesion characteristics is summarized in *Tables 2,3*. For the masses, the differences in shape, margin, internal enhancement, and kinetic curve on CEM and MRI between the benign and malignant lesions were all statistically significant (P<0.05). For NME, the differences in the distribution and kinetic curve on CEM and distribution, margin, and internal enhancement on MRI between the benign and malignant lesions were all statistically significant (P<0.05).

Comparison of curve types between CEM and MRI

The coincidence rate of the CEM and MRI enhancement curves was 86.1%, with 11.5% (24/208) being persistent curves, 31.2% (65/208) plateau curves, and 43.3% (90/208) washout curves; meanwhile, the enhancement curves of the remaining 13.9% (29/208) were inconsistent (*Table 4*). Cohen kappa coefficient of the enhancement curves of CEM and MRI was 0.768 (95% CI: 0.728–0.808; P<0.001), indicating substantial agreement.

ROC analysis and diagnostic performance

The CEM-KS [median 8, interquartile range (IQR) 5–9] in the malignant lesions was significantly higher than that in the benign lesions (median 3, IQR 2–5) (P<0.001). The MRI-KS (median 8, IQR 5–8) in malignant lesions was significantly higher than that in benign lesions (median 3, IQR 2–5) (P<0.001; *Table 1*).

The AUC was statistically higher for the CEM-KS (AUC =0.856; 95% CI: 0.801–0.901) than for the CEM-BI-RADS category assignment (AUC =0.776; 95% CI: 0.713–0.831) (P=0.047; *Figure 3*). The sensitivity of CEM-KS was lower than that of CEM-BI-RADS (96.1% *vs.* 100.0%; P=0.041), but the specificity of CEM-KS was significantly higher than that of the CEM-BI-RADS (69.6% *vs.* 10.7%; P<0.001).

The AUC was significantly higher for MRI-KS (AUC =0.841; 95% CI: 0.784–0.888) than for MRI-BI-RADS (AUC =0.752; 95% CI: 0.687–0.809) (P=0.015; *Figure 3*). The specificity of MRI-KS was significantly higher than that of MRI-BI-RADS (66.1% *vs.* 12.5%; P<0.001), but there was no significant difference between the sensitivity of BI-RADS and that of KS (99.3% *vs.* 96.1%; P=0.074).

The AUC of CEM-KS was not significantly different from that of MRI-KS (P=0.538). The sensitivity and specificity of CEM-KS and MRI-KS were 96.1% (146/152), 96.1% (146/152), 69.6% (39/56), and 66.1% (37/56), respectively. No significant differences were found between the sensitivity and specificity (P=0.617).

The difference between the AUCs of CEM-BI-RADS and MRI-BI-RADS was not statistically significant (0.776 *vs.* 0.752; P=0.400). There were no significant differences between the sensitivity and specificity of CEM-BI-RADS and MRI-BI-RADS (all P values =1.000).

The diagnostic sensitivity, specificity, PPV, NPV, +LR, and –LR are listed in *Table 5*. Examples of the CEM-KS and MRI-KS applications are shown in *Figures 4-6*.

Subgroup analyses

When the mass and NME were analyzed separately, the AUCs for the mass were 0.910 (95% CI: 0.851–0.951) and 0.903 (95% CI: 0.844–0.945) on CEM-KS and MRI-KS, and those for NME were 0.680 (95% CI: 0.549–0.794) and 0.621 (95% CI: 0.484–0.745). The CEM-KS and MRI-KS showed higher AUCs for mass than for NME (both P values <0.001). The AUCs for the larger-tumor-size (>2 cm)

Table 2 CEM enhancement features of benign and malignant lesions

Variable	Characteristic	Benign (n=56)	Malignant (n=152)	P
Mass		39	108	
Shape				<0.001
	Oval	8	5	
	Round	22	41	
	Irregular	9	62	
Margin				<0.001
	Circumscribed	30	23	
	Irregular	8	44	
	Spiculated	1	41	
Internal enhancement				0.001
	Homogeneous	20	22	
	Heterogeneous	14	68	
	Rim enhancement	5	18	
Kinetic curve				<0.001
	Persistent	13	2	
	Plateau	18	32	
	Washout	8	74	
NME		17	44	
Distribution				0.045
	Focal	12	22	
	Linear	0	2	
	Segmental	0	12	
	Regional	5	8	
Margin				0.425
	Irregular	13	39	
	Spiculated	4	5	
Internal enhancement				0.747
	Homogeneous	4	7	
	Heterogeneous	13	37	
Kinetic curve				0.028
	Persistent	7	5	
	Plateau	7	21	
	Washout	3	18	

CEM, contrast-enhanced mammography; NME, non-mass enhancement.

Table 3 MRI enhancement features of benign and malignant lesions

Variable	Characteristic	Benign (n=56)	Malignant (n=152)	P
Mass		40	110	
Shape				0.001
	Oval	8	10	
	Round	19	27	
	Irregular	13	73	
Margin				<0.001
	Circumscribed	30	20	
	Irregular	9	58	
	spiculated	1	32	
Internal enhancement				<0.001
	Homogeneous	15	5	
	Heterogeneous	21	87	
	Rim enhancement	4	18	
Kinetic curve				<0.001
	Persistent	13	2	
	Plateau	15	37	
	Washout	12	71	
NME		16	42	
Distribution				0.006
	Focal	12	16	
	Linear	0	1	
	Segmental	0	16	
	Regional	4	9	
Margin				<0.001
	Irregular	10	39	
	Spiculated	6	3	
Internal enhancement				0.003
	Homogeneous	1	2	
	Heterogeneous	15	23	
	Clustered ring	0	17	
Kinetic curve				0.068
	Persistent	7	6	
	Plateau	6	23	
	Washout	3	13	

MRI, magnetic resonance imaging; NME, non-mass enhancement.

Table 4 Comparison of enhancement curves between CEM and MRI

CEM	MRI			Total
	Type I	Type II	Type III	
Type I	24	3	0	27
Type II	4	65	9	78
Type II	0	13	90	103
Total	28	81	99	208

Type I, persistent; type II, plateau; type III, washout. CEM, contrast-enhanced mammography; MRI, magnetic resonance imaging.

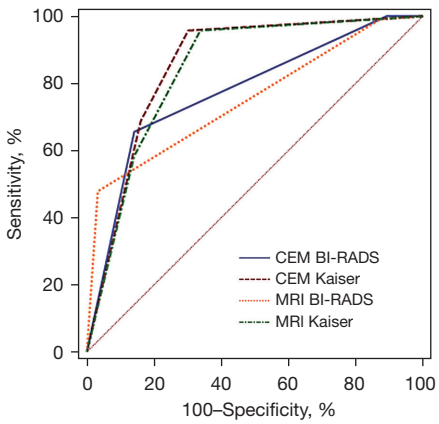

Figure 3 The ROC curves for CEM and MRI. CEM, contrast-enhanced mammography; BI-RADS, Breast Imaging Reporting and Data System; MRI, magnetic resonance imaging; ROC, receiver operating characteristic.

group were 0.934 (95% CI: 0.862–0.975) and 0.871 (95% CI: 0.785–0.932) on CEM-KS and MRI-KS, respectively, while those for the small-tumor-size (≤2 cm) group were 0.832 (95% CI: 0.752–0.895) and 0.835 (95% CI: 0.755–0.898), respectively. The CEM-KS showed a higher AUC for the larger-tumor-size group (P<0.001). The AUCs for postmenopausal group were 0.925 (95% CI: 0.847–0.971) and 0.924 (95% CI: 0.846–0.971) on CEM-KS and MRI-KS, respectively, while those for the premenopausal group were 0.838 (95% CI: 0.761–0.898) and 0.818 (95% CI: 0.739–0.882), respectively. The CEM-KS and MRI-KS showed higher AUCs for the postmenopausal group (P=0.036 and P=0.006, respectively).

The agreement between CEM-KS and MRI-KS

The kappa value for the characterization of suspicious breast lesions using CEM-KS and MRI-KS was 0.885 (P<0.001), indicating almost perfect agreement.

Cost-effectiveness analysis

CEM cost CNY ¥605 with a cost-effectiveness ratio of 706.775, while MRI cost CNY ¥1,478 with a cost-effectiveness ratio of 1,757.432. Therefore, CEM-KS is more cost-effective than is MRI-KS in differentiating between benign and malignant breast lesions.

Discussion

CEM, is an emerging imaging technology that can not only evaluate the morphological characteristics of lesions but also provide functional information from contrast absorption as a substitute for tumor neoangiogenesis in a similar fashion to breast MRI (25-27). However, the application of MRI is limited by the relatively high cost, low availability, and comparatively limited diagnostic efficiency of suspected calcification (27,28). CEM has gained attention due to its low examination cost, better accessibility than MRI, and improve diagnostic performance compared with mammography (25-29). In our study, we evaluated the potential of CEM-BI-RADS and CEM-KS for the differentiation of malignant and benign breast lesions and compared the results with those obtained with breast MRI, which revealed a comparable diagnostic performance between the modalities. CEM-KS and MRI-KS showed higher diagnostic performance than did CEM-BI-RADS and MRI-BI-RADS, respectively. The agreement between CEM and MRI for the diagnostic categories according to the KS was almost perfect, demonstrating that CEM-KS has the potential to serve as valuable indicator in the differentiation of breast lesions.

Several studies have reported the diagnostic value of MRI-KS in different clinical settings (8-11,14,15,18,19,30-33). Milos *et al.* (9) demonstrated that the KS could be used for patients with high-risk breast cancer who were recalled after their screening exams due to the detection of BI-RADS 4 breast lesions. This could obviate unnecessary benign biopsy, especially for those with enhancing lesions

Table 5 Diagnostic performance of KS and BI-RADS on CEM and MRI

Parameter	Sensitivity, % (95% CI)	Specificity, % (95% CI)	PPV, % (95% CI)	NPV, % (95% CI)	+LR, (95% CI)	−LR, (95% CI)
CEM						
BI-RADS	100 (96.9–100)	10.7 (4.4–22.6)	75.2 (68.6–80.9)	100 (51.6–100)	1.12 (1.02–1.23)	0
KS	96.1 (91.2–98.4)	69.6 (55.7–80.8)	89.6 (83.6–93.6)	86.7 (72.5–94.5)	3.16 (2.13–4.71)	0.06 (0.03–0.13)
MRI						
BI-RADS	99.3 (95.8–100)	12.5 (5.6–24.7)	75.5 (68.8–81.2)	87.5 (46.7–99.3)	1.14 (1.03–1.25)	0.05 (0.01–0.47)
KS	96.1 (91.2–98.4)	66.1 (52.1–77.8)	88.5 (82.4–92.7)	86.1 (71.4–94.2)	2.83 (1.96–4.09)	0.06 (0.03–0.13)

KS, Kaiser score; BI-RADS, Breast Imaging Reporting and Data System; CEM, contrast-enhanced mammography; MRI, magnetic resonance imaging; CI, confidence interval; PPV, positive predictive value; NPV, negative predictive value; +LR, positive likelihood ratio; −LR, negative likelihood ratio.

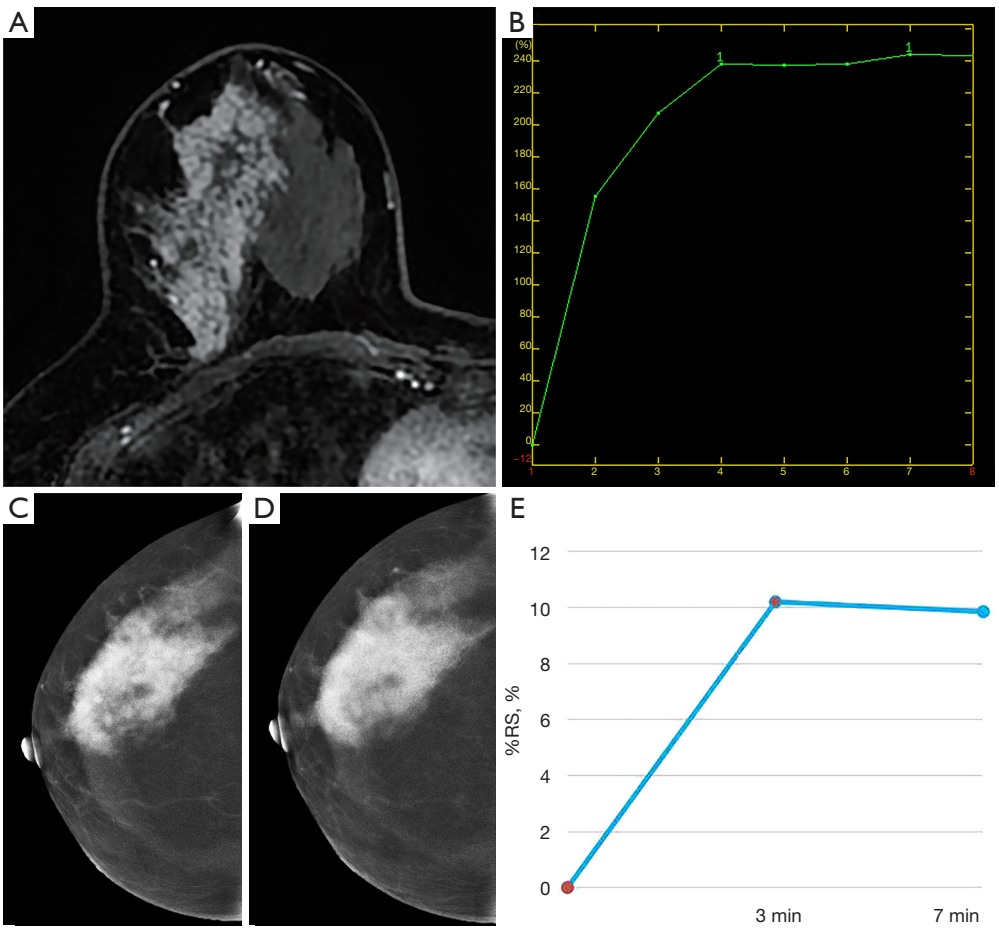

Figure 4 A 50-year-old patient with a ductal carcinoma in situ (high nuclear grade) with microinvasion. MRI early contrast-enhanced phase showed (A) a segmental NME lesion with irregular margin, clustered ring enhancement, and (B) a plateau time-signal intensity curve corresponding to a KS of 5. (C) Early and (D) late RC images on CEM demonstrated a segmental NME lesion with irregular margin, heterogeneous internal enhancement, and (E) a plateau curve also corresponding to a KS of 5. MRI, magnetic resonance imaging; NME, non-mass enhancement; KS, Kaiser score; RC, recombined; CEM, contrast-enhanced mammography.

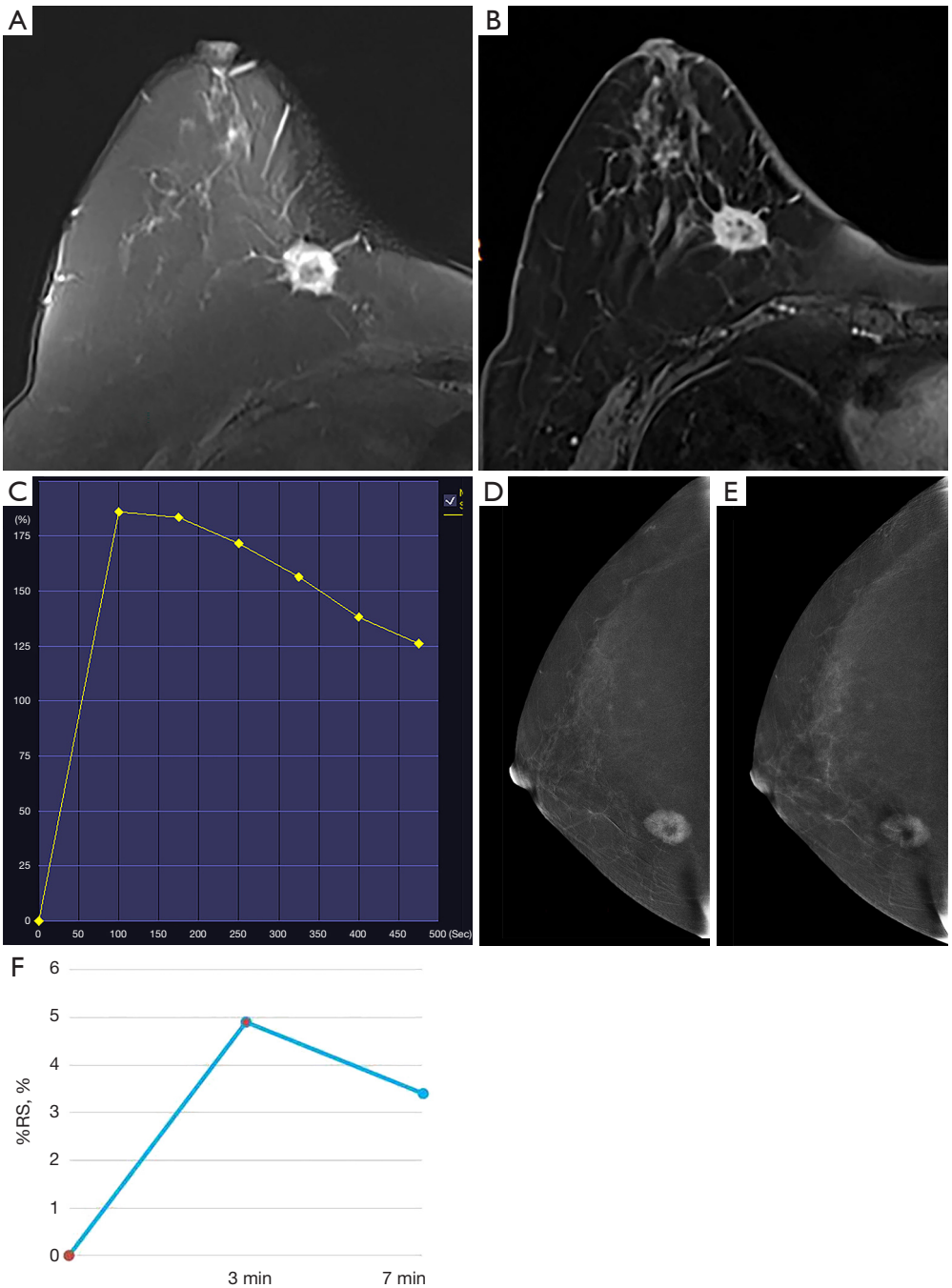

Figure 5 A 58-year-old patient with grade II invasive ductal carcinoma. (A) Perifocal edema was absent on T2WI. On MRI, the early contrast-enhanced phase showed (B) an irregular mass with spiculations, rim enhancement, and (C) a washout time-signal intensity curve corresponding to a KS of 9. (D) Early and (E) late RC images on CEM demonstrated an irregular mass with spiculations, rim enhancement, and (F) a washout curve also corresponding to a KS of 10. T2WI, T2-weighted imaging; MRI, magnetic resonance imaging; KS, Kaiser score; RC, recombined; CEM, contrast-enhanced mammography.

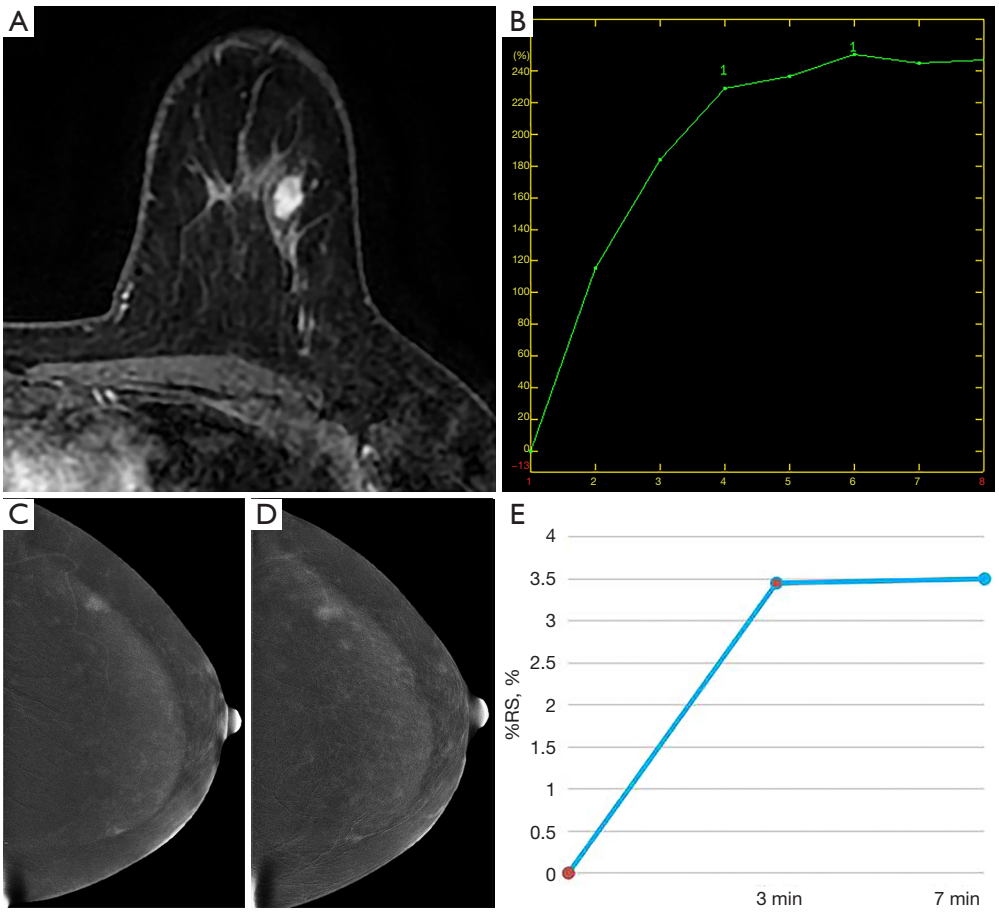

Figure 6 A 46-year-old patient with a fibroadenoma. On MRI, the early contrast-enhanced phase showed (A) an oval, circumscribed mass with heterogeneous internal enhancement and (B) a plateau time-signal intensity curve corresponding to a KS of 2. (C) Early and (D) late RC images on CEM demonstrated a circumscribed mass and (E) a plateau curve also corresponding to a KS of 2. MRI, magnetic resonance imaging; KS, Kaiser score; RC, recombined; CEM, contrast-enhanced mammography.

that presented as masses. Jajodia *et al.* (30) performed an analysis on MR using the KS for inconclusive or equivocal lesions on DM and found that applying the KS in patients undergoing MRI as a problem-solving tool could improve diagnostic sensitivity, specificity, and accuracy and avoid 45.2–60.8% of the unnecessary breast biopsies. Istomin *et al.* (14) investigated the diagnostic performance of the KS and compared it with that of multiparametric classification system (MCS) based on BI-RADS. They found that the KS had a slightly lower sensitivity. However, the specificity was 3–4 times greater than that of the MCS, which was similar to our study results. In addition, we found that the AUCs of MRI-KS for NME and the premenopausal group were significantly lower than those for masses and the postmenopausal group. The possible reasons for this are as follows: First, the evaluation of margin characteristics for NME was difficult as compared with those of masses. Second, background parenchymal enhancement (BPE) of the premenopausal group is typically strong, which may affect the accurate evaluation of lesion characteristics (34). The apparent diffusion coefficient (ADC) value is a promising quantitative biomarker in evaluating breast lesions. However, An *et al.* (19) assessed the ability of ADC values when combined with KS and found no additional value to KS for characterizing breast lesions. Due to the diversity of MRI equipment in our study, ADC values were not included in the analysis but will be incorporated in further in-depth studies.

To date, the evidence for CEM used with the KS is scarce, with only a few published studies (12,13). In a

recent study, we discovered that the CEM-KS had a high diagnostic performance in distinguishing benign from malignant breast lesions and outperformed CEM-BI-RADS; moreover, the KS yielded higher AUCs for mass than those for NME (13). In the present study, in addition to the results confirming our previous findings, we also compared the diagnostic performance of CEM-KS and MRI-KS for suspicious breast lesions and found that both techniques had similar diagnostic value and almost perfect agreement for the characterization of suspicious breast lesions. In addition, we also found that the AUCs of CEM-KS for the larger-tumor-size group and postmenopausal group were higher than those for the small-tumor-size and premenopausal group. Therefore, we can conclude that the patients in postmenopausal group, mass group, and larger tumor size group benefit more from CEM-KS.

Kinetic curves are the second most significant diagnostic criterion and play a crucial role in the assessment of KS (35). Recent studies (22,36-38) have shown that the CEM kinetic curve difference between benign and malignant breast lesions is significant. In their study, Deng *et al.* (36) found that the malignant lesions had more relatively depressed enhancement than did benign lesions. Ainakulova *et al.* (39) reported that CEM with delayed imaging had a higher specificity than did CEM without delayed imaging and that the plateau and washout curve were typical for malignancy. Froeling *et al.* (40) demonstrated that contrast-enhanced digital breast tomosynthesis showed significantly concordant agreement in terms of kinetics curves with MRI, which was consistent with our study, in which the agreement of the CEM and MRI enhancement curves was substantial.

The cost-effectiveness analysis showed that CEM-KS was more cost-effective than was MRI-KS in differentiating between benign and malignant breast lesions, which further suggests that CEM is worthy of clinical promotion and application.

Despite the promising findings, there are several limitations to our study that should be mentioned. First, we employed a retrospective and single-institution design, and a thus a prospective multicenter study will be performed to further verify our results. The retrospective design might also have promoted a certain degree of selection bias in choosing more suspicious cases. Nevertheless, this study represents the day-to-day practice in a specialized oncology tertiary hospital, and indeed, all consecutive patients were included in this study to reduce bias. Second, we did not determine the interobserver agreement for CEM-KS and MRI-KS; however, this related content has been studied in previous studies (8-15,18,19,30-32). Third, the MRI scans were performed on different devices with distinct field strengths and scanning parameters. This was unavoidable, as the patients in our study were retrospectively recruited. On the other hand, the limitation could also be taken as a strength because this confirmed the universal applicability of the KS, which could be applied to various MRI protocols and systems. Finally, BPE affects the display of the lesion margin and measurement of kinetic curves, thereby potentially affecting diagnostic performance of CEM-KS; this effect will be considered in future studies.

Conclusions

The preliminary results of our study show that the KS substantially improves the diagnostic performance for suspicious breast lesions, thus potentially decreasing unnecessary biopsies and patient discomfort, not only in MRI but also in CEM. CEM-KS and MRI-KS have similar diagnostic performance and almost perfect agreement for the characterization of breast lesions. Furthermore, CEM-KS is more cost-effective than is MRI-KS in differentiating between benign and malignant breast lesions. Therefore, CEM holds promise as alternative to MRI when it is not available or is contraindicated.

Acknowledgments

The abstract of this paper was published in the 2023 Annual Breast Imaging Conference of the Chinese Society of Radiology.
Funding: None.

Footnote

Reporting Checklist: The authors have completed the STARD reporting checklist. Available at https://qims.amegroups.com/article/view/10.21037/qims-24-593/rc

Conflicts of Interest: All authors have completed the ICMJE uniform disclosure form (available at https://qims.amegroups.com/article/view/10.21037/qims-24-593/coif). The authors have no conflicts of interest to declare.

Ethical Statement: The authors are accountable for all aspects of the work in ensuring that questions related to the accuracy or integrity of any part of the work are appropriately investigated and resolved. This study was

conducted in accordance with the Declaration of Helsinki (as revised in 2013) and was approved by ethics committee of The Fourth Hospital of Hebei Medical University (No. 2020ky182). Individual consent for this retrospective analysis was waived.

References

1. Sung H, Ferlay J, Siegel RL, Laversanne M, Soerjomataram I, Jemal A, Bray F. Global Cancer Statistics 2020: GLOBOCAN Estimates of Incidence and Mortality Worldwide for 36 Cancers in 185 Countries. CA Cancer J Clin 2021;71:209-49.
2. Fallenberg EM, Schmitzberger FF, Amer H, Ingold-Heppner B, Balleyguier C, Diekmann F, Engelken F, Mann RM, Renz DM, Bick U, Hamm B, Dromain C. Contrast-enhanced spectral mammography vs. mammography and MRI - clinical performance in a multi-reader evaluation. Eur Radiol 2017;27:2752-64.
3. Kim EY, Youn I, Lee KH, Yun JS, Park YL, Park CH, Moon J, Choi SH, Choi YJ, Ham SY, Kook SH. Diagnostic Value of Contrast-Enhanced Digital Mammography versus Contrast-Enhanced Magnetic Resonance Imaging for the Preoperative Evaluation of Breast Cancer. J Breast Cancer 2018;21:453-62.
4. Clauser P, Baltzer PAT, Kapetas P, Hoernig M, Weber M, Leone F, Bernathova M, Helbich TH. Low-Dose, Contrast-Enhanced Mammography Compared to Contrast-Enhanced Breast MRI: A Feasibility Study. J Magn Reson Imaging 2020;52:589-95.
5. Shahraki Z, Ghaffari M, Nakhaie Moghadam M, Parooie F, Salarzaei M. Preoperative evaluation of breast cancer: Contrast-enhanced mammography versus contrast-enhanced magnetic resonance imaging: A systematic review and meta-analysis. Breast Dis 2022;41:303-15.
6. Xing D, Lv Y, Sun B, Xie H, Dong J, Hao C, Chen Q, Chi X. Diagnostic Value of Contrast-Enhanced Spectral Mammography in Comparison to Magnetic Resonance Imaging in Breast Lesions. J Comput Assist Tomogr 2019;43:245-51.
7. Ferranti FR, Vasselli F, Barba M, Sperati F, Terrenato I, Graziano F, Vici P, Botti C, Vidiri A. Diagnostic Accuracy of Contrast-Enhanced, Spectral Mammography (CESM) and 3T Magnetic Resonance Compared to Full-Field Digital Mammography plus Ultrasound in Breast Lesions: Results of a (Pilot) Open-Label, Single-Centre Prospective Study. Cancers (Basel) 2022;14:1351.
8. Wengert GJ, Pipan F, Almohanna J, Bickel H, Polanec S, Kapetas P, Clauser P, Pinker K, Helbich TH, Baltzer PAT. Impact of the Kaiser score on clinical decision-making in BI-RADS 4 mammographic calcifications examined with breast MRI. Eur Radiol 2020;30:1451-9.
9. Milos RI, Pipan F, Kalovidouri A, Clauser P, Kapetas P, Bernathova M, Helbich TH, Baltzer PAT. The Kaiser score reliably excludes malignancy in benign contrast-enhancing lesions classified as BI-RADS 4 on breast MRI high-risk screening exams. Eur Radiol 2020;30:6052-61.
10. Dietzel M, Krug B, Clauser P, Burke C, Hellmich M, Maintz D, Uder M, Bickel H, Helbich T, Baltzer PAT. A Multicentric Comparison of Apparent Diffusion Coefficient Mapping and the Kaiser Score in the Assessment of Breast Lesions. Invest Radiol 2021;56:274-82.
11. Marino MA, Clauser P, Woitek R, Wengert GJ, Kapetas P, Bernathova M, Pinker-Domenig K, Helbich TH, Preidler K, Baltzer PA. A simple scoring system for breast MRI interpretation: does it compensate for reader experience? Eur Radiol 2016;26:2529-37.
12. Rong X, Kang Y, Xue J, Han P, Li Z, Yang G, Shi G. Value of contrast-enhanced mammography combined with the Kaiser score for clinical decision-making regarding tomosynthesis BI-RADS 4A lesions. Eur Radiol 2022;32:7439-47.
13. Kang Y, Li Z, Yang G, Xue J, Zhang L, Rong X. Diagnostic performance of the Kaiser score in the evaluation of breast lesions on contrast-enhanced mammography. Eur J Radiol 2022;156:110524.
14. Istomin A, Masarwah A, Vanninen R, Okuma H, Sudah M. Diagnostic performance of the Kaiser score for characterizing lesions on breast MRI with comparison to a multiparametric classification system. Eur J Radiol 2021;138:109659.
15. Woitek R, Spick C, Schernthaner M, Rudas M, Kapetas P, Bernathova M, Furtner J, Pinker K, Helbich TH, Baltzer PAT. A simple classification system (the Tree flowchart) for breast MRI can reduce the number of unnecessary biopsies in MRI-only lesions. Eur Radiol 2017;27:3799-809.

16. Mercado CL. BI-RADS update. Radiol Clin North Am 2014;52:481-7.
17. Baltzer PA, Dietzel M, Kaiser WA. A simple and robust classification tree for differentiation between benign and malignant lesions in MR-mammography. Eur Radiol 2013;23:2051-60.
18. Meng L, Zhao X, Lu L, Xing Q, Wang K, Guo Y, Shang H, Chen Y, Huang M, Sun Y, Zhang X. A Comparative Assessment of MR BI-RADS 4 Breast Lesions With Kaiser Score and Apparent Diffusion Coefficient Value. Front Oncol 2021;11:779642.
19. An Y, Mao G, Ao W, Mao F, Zhang H, Cheng Y, Yang G. Can DWI provide additional value to Kaiser score in evaluation of breast lesions. Eur Radiol 2022;32:5964-73.
20. Dietzel M, Baltzer PAT. How to use the Kaiser score as a clinical decision rule for diagnosis in multiparametric breast MRI: a pictorial essay. Insights Imaging 2018;9:325-35.
21. Lee CH, Phillips J, Sung JS, Lewin JM, Newell MS. ACR BI-RADS® contrast enhanced mammography (A supplement to ACR BI-RADS® mammography 2013). American College of Radiology, Reston, VA, 2022.
22. Liu Y, Zhao S, Huang J, Zhang X, Qin Y, Zhong H, Yu J. Quantitative Analysis of Enhancement Intensity and Patterns on Contrast-enhanced Spectral Mammography. Sci Rep 2020;10:9807.
23. Rudnicki W, Heinze S, Niemiec J, Kojs Z, Sas-Korczynska B, Hendrick E, Luczynska E. Correlation between quantitative assessment of contrast enhancement in contrast-enhanced spectral mammography (CESM) and histopathology-preliminary results. Eur Radiol 2019;29:6220-6.
24. Edwards SD, Lipson JA, Ikeda DM, Lee JM. Updates and revisions to the BI-RADS magnetic resonance imaging lexicon. Magn Reson Imaging Clin N Am 2013;21:483-93.
25. Ghaderi KF, Phillips J, Perry H, Lotfi P, Mehta TS. Contrast-enhanced Mammography: Current Applications and Future Directions. Radiographics 2019;39:1907-20.
26. Mann RM, Hooley R, Barr RG, Moy L. Novel Approaches to Screening for Breast Cancer. Radiology 2020;297:266-85.
27. Mann RM, Cho N, Moy L. Breast MRI: State of the Art. Radiology 2019;292:520-36.
28. Bennani-Baiti B, Baltzer PA. MR Imaging for Diagnosis of Malignancy in Mammographic Microcalcifications: A Systematic Review and Meta-Analysis. Radiology 2017;283:692-701.
29. Phillips J, Miller MM, Mehta TS, Fein-Zachary V, Nathanson A, Hori W, Monahan-Earley R, Slanetz PJ. Contrast-enhanced spectral mammography (CESM) versus MRI in the high-risk screening setting: patient preferences and attitudes. Clin Imaging 2017;42:193-7.
30. Jajodia A, Sindhwani G, Pasricha S, Prosch H, Puri S, Dewan A, Batra U, Doval DC, Mehta A, Chaturvedi AK. Application of the Kaiser score to increase diagnostic accuracy in equivocal lesions on diagnostic mammograms referred for MR mammography. Eur J Radiol 2021;134:109413.
31. Chen ZW, Zhao YF, Liu HR, Zhou JJ, Miao HW, Ye SX, He Y, Liu XM, Su MY, Wang MH. Assessment of breast lesions by the Kaiser score for differential diagnosis on MRI: the added value of ADC and machine learning modeling. Eur Radiol 2022;32:6608-18.
32. Wang Q, Fu F, Chen Y, Yang D, Zhang J, Yu H, Su L. Application of the Kaiser score by MRI in patients with breast lesions by ultrasound and mammography. Diagn Interv Radiol 2022;28:322-8.
33. Pötsch N, Korajac A, Stelzer P, Kapetas P, Milos RI, Dietzel M, Helbich TH, Clauser P, Baltzer PAT. Breast MRI: does a clinical decision algorithm outweigh reader experience? Eur Radiol 2022;32:6557-64.
34. Wang H, Gao L, Chen X, Wang SJ. Quantitative evaluation of Kaiser score in diagnosing breast dynamic contrast-enhanced magnetic resonance imaging for patients with high-grade background parenchymal enhancement. Quant Imaging Med Surg 2023;13:6384-94.
35. Grippo C, Jagmohan P, Helbich TH, Kapetas P, Clauser P, Baltzer PAT. Correct determination of the enhancement curve is critical to ensure accurate diagnosis using the Kaiser score as a clinical decision rule for breast MRI. Eur J Radiol 2021;138:109630.
36. Deng CY, Juan YH, Cheung YC, Lin YC, Lo YF, Lin G, Chen SC, Ng SH. Quantitative analysis of enhanced malignant and benign lesions on contrast-enhanced spectral mammography. Br J Radiol 2018;91:20170605.
37. Huang JS, Pan HB, Yang TL, Hung BH, Chiang CL, Tsai MY, Chou CP. Kinetic patterns of benign and malignant breast lesions on contrast enhanced digital mammogram. PLoS One 2020;15:e0239271.
38. Xu W, Zheng B, Chen W, Wen C, Zeng H, He Z, Qin G, Li Y. Can the delayed phase of quantitative contrast-enhanced mammography improve the diagnostic performance on breast masses? Quant Imaging Med Surg 2021;11:3684-97.
39. Ainakulova AS, Zholdybay ZZ, Kaidarova DR, Inozemtceva NI, Gabdullina MO, Zhakenova ZK, Panina AS, Toleshbayev DK, Amankulov JM. Contrast-enhanced

spectral mammography without and with a delayed image for diagnosing malignancy among mass lesions in dense breast. Contemp Oncol (Pozn) 2021;25:17-22.
40. Froeling V, Diekmann F, Renz DM, Fallenberg EM, Steffen IG, Diekmann S, Lawaczeck R, Schmitzberger FF. Correlation of contrast agent kinetics between iodinated contrast-enhanced spectral tomosynthesis and gadolinium-enhanced MRI of breast lesions. Eur Radiol 2013;23:1528-36.

Cite this article as: Rong X, Kang Y, Li Y, Xue J, Li Z, Yang G. Application of the Kaiser score on contrast-enhanced mammography in the differential diagnosis of breast lesions: comparison with breast magnetic resonance imaging. Quant Imaging Med Surg 2024;14(8):5541-5554. doi: 10.21037/qims-24-593

